DISSERTATION

On

Target Reaching and Workspace Analysis of a Planar Parallel Manipulator

Submitted in partial fulfillment of the requirement for the award of degree

of

Master of Engineering

IN

CAD/CAM Engineering

Submitted by

Dharmveer Agarwal

Registration No.: 801481009

Under the guidance of

Dr. TARUN KUMAR BERA

Associate Professor

Department of Mechanical Engineering

Thapar University, Patiala

DEPARTMENT OF MECHANICAL ENGINEERING

THAPAR UNIVERSITY

PATIALA-147004, INDIA

JULY-2016

DECLARATION

*I hereby declare that work done in the thesis report entitled, "**Target Reaching and Workspace Analysis of a Planar Parallel Manipulator**" submitted towards partial fulfillment of requirement for award of **Master of Engineering degree** in **CAD/CAM Engineering** in Mechanical Engineering Department of Thapar University, Patiala, is an authentic record of work carried out by me under the supervision and guidance of **Dr. Tarun Kumar Bera**, Associate Professor of Mechanical Engineering Department, Thapar University, Patiala.*

Dharmveer Agarwal,

(Dharmveer Agarwal)

This is to certify that above declaration made by the student concerned is correct to the best of my knowledge and belief.

Tarun Kumar Bera 15/7/16

(Dr. Tarun Kumar Bera)

Associate Professor

Mechanical Engineering Department

Thapar University, Patiala

Countersigned by:

Head of Mechanical Engineering Department
Thapar University, Patiala

Dean of Academic Affairs
Thapar University, Patiala

ACKNOWLEDGEMENTS

I would like to express my deep sense of gratitude to my supervisor Dr. Tarun Kumar Bera, Associate Professor, Mechanical Engineering Department, Thapar University, Patiala for his uninterrupted guidance, constructive suggestions and overwhelming inspiration in guiding my research work. It was an enriching and pleasing experience working with him.

I am grateful to my mother and guardian Smt. Krishna Agarwal for enduring support and mentorship. I am also thankful to my peers Kartik Sharma, Abhay Singh Rana and Rashmi Arora for their fruitful discussions and constructive suggestions.

Finally, I express my sincere gratitude to university administration and staffs to enable me complete my thesis report.

Dharmveer Agarwal.

(Dharmveer Agarwal)

Registration No.: 801481009

ABSTRACT

Parallel manipulators due to their higher load carrying capacity, high precision and stiffness are increasingly becoming popular in industry and research. Integration of automatic control system has enabled parallel manipulators to perform tasks which were hitherto not possible. This opens endless vistas for research work in the field of parallel manipulators. Areas such as machining, welding, trajectory tracking are being explored. This dissertation is a continuation of this legacy. In this present work, an electrically actuated manipulator leg based on ball screw feed drive has been modelled. A 3-DOF parallel planar manipulator with ball screw feed drive legs is modelled. An inversion controller using overwhelming control for trajectory tracking purposes is developed. Thereafter, another inversion controller based on proportional control is developed. Simulation of the bond graph models have been carried out on SYMBOLS Shakti software. Workspace analysis plays a cardinal role in the trajectory planning, design and operation of a manipulator. Workspace analysis corresponding to the trajectory tracking manipulator is carried out. Constant orientation workspace based upon constraints on actuated and unactuated joints is determined. The required workspace is obtained with the help of MATLAB.

Keywords: Planar parallel manipulator, trajectory tracking, target reaching, workspace analysis, bond graph

LIST OF ABBREVIATIONS

C	Compliance element
DOF	Degrees of freedom
GY	Gyrator element
I	Inertial element
R	Resistance element
SE	Source of flow
SF	Source of effort
TF	Transformer element

NOMENCLATURE

AB	Length of platform
CDE	Length of fixed base
C_n	Damping of nut
C_{sa}	Damping of axial component of shaft
C_{sr}	Damping of rotational component of shaft
d	Equivalent diameter of shaft
E	Young's modulus of shaft
G	Shear modulus of the shaft
G_x	Gain along x-axis
G_y	Gain along y-axis
i	Transmission ratio
J_m	Motor rotary inertia
J_P	Platform rotary inertia
J_s	Shaft rotary inertia
K_a	Overall axial stiffness
K_b	Bearing axial stiffness
K_c	Coupling rotational stiffness
K_n	Stiffness of nut
K_r	Overall rotational stiffness
K_{sa}	Stiffness of rotational component of shaft
K_{sr}	Stiffness of rotational component of shaft
l	Length of the shaft
l_{ac}	Actuator length
m_s	Shaft mass
m_t	Link mass
M_P	Platform mass
T	Motor torque
θ_1	Rotation of motor

θ_2	Rotation of shaft
ϕ	Platform orientation
ρ	Density of the shaft
μ_{H}	High gain
μ_{L}	Low gain

SUBSCRIPTS

H	High
L	Low
G	Centre of gravity
t	Link
s	Shaft
m	Motor
sa	Axial component of shaft
sr	Rotational component of shaft
ac	Actuator
vel	Velocity

LIST OF FIGURES

LIST OF TABLES

TABLE OF CONTENTS

Chapter 1 Introduction

This chapter deals with the introduction of the various topics and concepts based upon which dissertation is carried out. The chapter begins with the background and motivation and introduction of robotic manipulators. Thereafter, basic concepts of ball screw feed drive, control system for trajectory tracking and target reaching and workspace analysis are discussed. Modelling of physical systems using bond graph technique is also discussed. This chapter concludes with the contribution and organization of the thesis.

1.1 Background and Motivation

Control systems are increasingly being used in day to day life for industrial as well as for personal usages. Parallel manipulators are increasing becoming popular for their higher load carrying capacity, stiffness *etc*. As a result, now-a-days parallel manipulators have come equipped with control systems capable of solving complex algorithms/calculations and handling various tasks which were hitherto not possible with required efficiency and accuracy. This opens endless vistas for exploration and research in the fields of machining, welding, heavy industrial and space applications, trajectory tracking or a mere pick and place application. Not only trajectory tracking of parallel manipulator is important but also target reaching for workspace analysis is a challenging task for this type of manipulator.

1.2 Robotic Manipulators

A robotic manipulator is an electro-mechanical device consisting of rigid links connected by joints capable of manipulating physical objects in its workspace. Manipulators can be classified according to several criteria such as on the basis of drive technology as electric, hydraulic and pneumatic manipulators, on the basis of work-envelope geometry as Cartesian, cylindrical, spherical, SCARA and articulated manipulators, on the basis of motion control methods as point to point and continuous path motion. Another important classification is on the basis of kinematic structure as serial manipulators, parallel manipulators and hybrid manipulators.

Serial manipulators also known as open loop manipulators are the ones whose kinematic structure takes the shape of an open loop with one link fixed to the ground and the last link connected to the end effectors. Parallel manipulators are the ones whose kinematic structure takes the shape of a closed loop. All the links are simultaneously joined to the base as well as to

the end effectors. Hybrid manipulators are the ones having properties of both open loop and closed loop chains.

1.3 Linear Actuators

A linear actuator is a device which generates linear motion. They find wide applications in industry especially where linear motion is required. Linear actuators can be basically categorized as Mechanical actuators, hydraulic actuators, pneumatic actuators and electro-mechanical actuators. Hydraulic and pneumatic actuators employ pressurized fluid and air respectively to generate motion whereas electro-mechanical actuators are actuated by electric current. Mechanical actuators usually operate by converting rotational velocity into linear velocity. This is done through simple mechanisms such as screw, wheel and axle, cam *etc*.

The mechanical linear actuators working on screw mechanism are ball screw, lead screw, screw jack and roller screw. Ball screw is a rolling contact mechanical linear actuator in which steel balls housed in a nut roll over to generate motion. Due to rolling friction ball screw has low wear leading to low cost maintenance, reduced lubrication and high mechanical efficiency. They are also capable of converting linear motion in rotary motion. Lead screws are similar to ball screws except that sliding friction replaces rolling friction and the nut is in direct contact with the screw eliminating the necessity of balls. Although, the mechanical efficiency of lead screws is not good nonetheless they are easy to manufacture and can carry high loads with fair amount of precision.

1.4 Control System

A Control system is essentially a combination of elements arranged in such a manner so as to create the desired output. Control systems may be broadly categorized as Open loop and Closed loop control systems. An open loop control system is the one in which the output solely depends on the input whereas in a closed loop system the output is fed back so as to facilitate required control action for generating the desired output. Closed loop control systems are also known as Feedback control systems. Proportional control and overwhelming control are two of the major control actions employed in control systems.

In Proportional control, the actuating signal is proportional to the error signal which is the difference between the reference and the feedback signal. Increasing the gain of proportional

control reduces the settling time and steady state error but at the same time increases the maximum overshoot. In an overwhelming control, the controller mass M^* is rigidly attached to the plant mass in physical domain and the plant dynamics are completely overwhelmed by the controller dynamics by the application of a high gain, $\mu_H >> 1$ at the same maintaining the similarity of motion with the plant by the application of a low gain, $\mu_L = 1$.

1.5 Trajectory Tracking

Trajectory tracking can be described as replication of a reference trajectory by the end effectors of the manipulator. Trajectory tracking finds wide applications in the world of manipulators ranging from machining, finishing and welding to a simple pick and place application. Replication of the input along given coordinates with negligible errors form the basic characteristic of a trajectory tracking system.

1.6 Target Reaching

Target reaching is the event of the end effectors of the manipulator arriving or reaching at a given target. The target is usually fed in terms of its coordinates and the manipulator is required to reach the given target irrespective of the path traversed to reach it. The basic characteristic of a target reaching system is reaching at the given target with negligible errors.

1.7 Workspace Analysis

Workspace may be described as the locus of all points which are reachable by the end effectors of the manipulator. Workspace may also be categorized as Maximal workspace, Constant orientation workspace and Dexterous workspace. Maximal workspace or Total workspace is the locus of all points reachable by at least one orientation. Constant orientation workspace is the locus of all points reachable by a given fixed orientation whereas Dexterous workspace is the locus of all points reachable by any orientation of the end effectors of the manipulator.

1.8 Bond Graph Modelling

A bond graph may be described as the pictorial representation of the energy interaction between the subsystems of a system. The beauty of bond graph modelling is that it can be used to model systems having subsystems in different energy domains be it mechanical, electrical, thermal or hydraulic subsystem. This is achieved by segregating the power variables of every energy domain in two types, Effort and Flow. A bond graph consists of single, double and multi port

elements connected by bonds which carry power from one element to another through 0 and 1-junctions. I, C, R, SE and SF are the five single port elements. Inertances, compliances and dissipaters are represented by I, C and R elements respectively whereas SE and SF elements represent source of effort and source of flow respectively. TF and GY are two double port elements representing Transformer and Gyrator elements. Whereas TF element denotes the magnification of power variables, GY element denotes change in the nature of power variable together with magnification. Junctions 0 and 1 decide the nature of interaction between various elements i.e. common flow and common effort. Bond graph modelling technique finds wide acceptance in modeling dynamic systems especially multi body and mechatronic systems.

1.9 Contribution of the Thesis

The contributions of this thesis are as follows:

- Literature review pertaining to parallel manipulator is carried out.
- Bond graph model of ball screw feed drive is developed.
- Bond graph model of a parallel planar manipulator using ball screw feed drives as its leg is developed.
- An inversion controller using overwhelming control for trajectory tracking purposes is developed.
- Another inversion controller based on Proportional control for target reaching purposes is developed.
- Workspace analysis associated with the trajectory tracking manipulator is carried out.

1.10 Organization of the Thesis

This thesis is organized in five chapters which are summarized as:

Chapter 1: It deals with the introduction of the various topics and concepts based upon which dissertation is carried out. The chapter begins with the introduction of Parallel manipulators. Thereafter, basic concepts of ball screw feed drive, controllers, trajectory tracking, target reaching and workspace analysis are discussed. Modelling of physical systems using bond graph technique is also discussed. The chapter concludes with contribution and organization of the thesis.

Chapter 2: This chapter summarizes the topic wise literature review carried out for the dissertation work. The review is done in the areas of Parallel manipulator, ball screw and workspace analysis. The literature gap and objectives of the thesis are presented at end of the chapter.

Chapter 3: This chapter deals with a parallel planar manipulator employed for trajectory tracking purposes. Modelling of the manipulator is followed by the results obtained through simulation.

Chapter 4: This chapter deals with the modelling and simulation of a parallel planar manipulator employed for target reaching purposes. Workspace analysis corresponding to the trajectory tracking manipulator is also carried out.

Chapter 5: It provides the conclusions drawn from the dissertation of the thesis and suggests scope for future research work.

Chapter 2 Literature Review

This chapter deals with the literature review done as part of thesis dissertation. The literature survey is done in the areas of parallel manipulators, workspace analysis and bond graph modeling technique. The literature gap identified and objectives of the thesis are presented at the end of the chapter.

2.1 Literature Survey

2.1.1 Literature Survey on Parallel Manipulators

A parallel manipulator may be described as a closed kinematic chain in which the end effector is connected to the base through numerous independent kinematic chains. They have high rigidity and precision as opposed to serial manipulators which have larger workspace. Another problem with serial manipulator is that their end effectors tend to bend under high loads. This coupled with vibrations under high speed lead to poor accuracy. The applications of parallel manipulators include material handling, machine tools and welding. Other applications include surgery, painting, inspection, deep sea maintenance *etc*. Their main advantages are high load carrying capacity, low inertia and high accuracy. Their disadvantages are small workspace, small range of motion of joints and actuators and singularities [**1**].

Stewart platform, one of the most famous parallel manipulator is a 6-DOF manipulator consisting of a platform supported by six prismatic legs that are connected to the ground and to the platform through universal and spherical unactuated joints. Stewart manipulator which is also used as a flight simulator demonstrates duality against serial manipulators. Contrary to serial manipulators the forward kinematics of parallel manipulators are difficult to determine whereas the inverse kinematics can be found out in an easier manner. It is found that the workspace and maneuvering capability of the platform is low. It can be used as a force sensor as well [**2**]. Dynamic characteristics of a manipulator are cardinal for control system design. A full model of Stewart platform is difficult to deal with. Hence, a reduced model neglecting the linear motor dynamics was developed and found to work efficiently [**3**].

The topology of a manipulator may be broadly described as its kinematic composition together with required constraints. It provides an insight as to which links are connected to whom and with what types of joints. Topology is dimensionally independent. Although planar

manipulators can be described but owing to lack of dimensional information, spatial manipulators are difficult to describe in topology. This was overcome by introducing some essential constraints after the analysis of architecture representing the manipulator [**4**].

Natural frequency and stiffness play key role in defining the capabilities of manipulators. In case of machine tools they allow higher cutting speeds and feeds with desired surface finish and tool life. It was observed that the natural frequency and stiffness of a 3-DOF parallel manipulator increased with addition of a redundant leg actuator to the manipulator. Nonetheless no appreciable increase in frequency and stiffness were found after the addition of second leg actuator [**5**].

In reference [**6**], an overwhelming control based inversion controller is developed for a 3-DOF parallel planar manipulator. The manipulator consists of a platform supported by electro-hydraulic actuated legs which are connected to the fixed base and to the platform with unactuated revolute joints. The leg is modelled considering the dynamics of a cylinder and servo-valve. The controller owing to overwhelming control is able to compensate for the unidentified parameters as well hence making the system robust. The entire modelling is done with bond graph. The input to the controller is provided from a planar vehicle simulator as a test case. The controller generated the required forces for the actuator legs to replicate the input motion. Heave and pitch motions of the vehicle simulator and as traced by the platform were compared and were found to be similar within given error limits. Similarly, Trajectory control of space robots based on overwhelming control was also developed. The space manipulator under consideration is a 3-DOF floating serial manipulator mounted on a satellite. Simulation carried out validated the robustness of the model [**7**].

Apart from trajectory control trajectory planning has also been explored and carried out so as to minimize the motion time, power consumed, for obstacle avoidance *etc* [**8-9**].

2.1.2 Literature Survey on Workspace Analysis

Workspace may be broadly defined as the volume that can be reached or covered by the end effectors of a manipulator. The volume consisting of all the points that could be reached with at least one orientation is known as *reachable workspace*. The volume within which every single point can be reached with a constant orientation of the end effectors is called *constant orientation workspace*. *Dexterous workspace* is the volume that can be reached with any given

orientation of the end effector. It follows that the union of all the constant orientation workspaces gives the reachable workspace whereas the intersection of all the constant orientation workspaces gives the dexterous workspace of a manipulator [**10**].

Workspace analysis is not a generalized technique. Methodology for determination of the workspace depends on the structure of the manipulator and its kinematics. Several literatures have been written on workspace analysis demonstrating different methodologies to achieve the same. A parallel planar manipulator with 3-DOF has been considered for workspace analysis in [**11**]. The manipulator consists of a moving platform which is connected to the fixed base with three prismatic legs. The legs are connected to the platform and to the base with unactuated revolute joints. The joints being revolute allow the platform to move only in a single plane. An inertial coordinate frame is attached to the ground whereas another non inertial frame is attached to the platform. It was observed that the sole effect of the motion of a leg on the centre of gravity of the end effector was to move it in a circle around a fixed centre. If minimum and maximum lengths of the leg are considered then the area swept will be an annular region about the fixed centre. Similarly, two more annular regions will be swept corresponding to the other two legs. The common region of these three annular regions will give the workspace without any limits on the revolute joints. The imposition of revolute joints will create sectors on each annular region corresponding to actuator legs. The required workspace is given by the intersection of the three sectored annular regions. Algorithms for the determination of the different kinds of workspaces for the same manipulator have been presented in [**12**].

Workspace analysis for another 3-DOF parallel planar manipulator has been done in [**13**]. The manipulator under consideration consists of a moving platform which is connected to the ground through three independent chains. Each chain consists of a prismatic actuator leg fixed to the ground. Another link is connected to the actuator leg and to the platform with unactuated revolute joints. An inertial frame is attached to the ground whereas another non inertial frame is attached to the platform. It was observed that the sole effect of the motion of a leg on the centre of gravity of the end effector was to move it in region bounded by two parallel lines on two sides and joined by two circular arcs on the remaining two sides. Similarly, two more regions are swept corresponding to the other two legs. The required workspace is obtained by the intersection of the three regions corresponding to the three actuator legs.

Workspace of a 6-DOF parallel manipulator has been determined in [**14**]. The manipulator consists of a moving platform connected to the fixed base with six independent chains. Each chain consists of a prismatic actuator leg connected to the platform and to the base with unactuated revolute joints. An inertial frame is attached to the ground whereas another non inertial frame is attached to the platform. It was observed that the sole effect of the motion of a leg on the centre of gravity of the end effector was to move it on the surface of a sphere. If minimum and maximum lengths of the leg are considered then the area swept will be an annular region between two spheres about the fixed centre. The common region of these six annular regions will give the workspace without any limits on the revolute joints. The required workspace is the common region obtained by the intersection of the six regions. The workspace in 3-dimensional space can also be visualized in a two dimensional space by taking a section of the workspace in a plane.

Parallel manipulators as known have limited workspace. This is overcome by the introduction of series-parallel hybrid manipulators in which two or more parallel structures are put in cascade. The workspace of hybrid and similar manipulators has been determined in [**15-17**].

2.1.3 Literature Survey on Bond Graph Modelling

Modelling of a system consists of identifying the system limits with respect to physical dimensions, frequency range *etc.,* segregation of the larger system into smaller subsystems and describing the physical relations between the subsystems as per the energy interactions taking place between them. A basic but challenging task is the identification of the state variables [**18**]. As such Bond graph modelling is increasingly gaining popularity among the researchers for modelling purposes.

Bond graph modelling technique was developed by Prof. Henry Paynter. A bond graph is a pictorial representation using power bonds to represent the energy interactions between the subsystems of a larger system. The beauty of bond graph is that the systems having subsystems in different energy domains can also be modelled. As the dynamic equations are expressed in state representations, bond graph approach comes handy in solving control design problems [**19**].

Bond graphs have been extensively used for modelling different kinds of systems. An underwater single degree of freedom robotic manipulator was modelled in reference [**20**]. The

arm of the manipulator was assumed to be a Raleigh beam. As the environment underwater is different from the one on ground, hydrostatic, hydrodynamic and buoyant forces were also taken into consideration. The dynamic behavior of the manipulator was analyzed and deflection of the arm was obtained.

Bond graph modelling technique has been applied to model a four wheeled vehicle to optimize the yaw rate of an under-steering vehicle for safety purpose. A non linear dynamic model with electrically controlled steering and brakes was developed. Controls were also provided at each suspension corner. These sub systems were modelled separately and then assembled to present the entire system for simulation. Yaw response of uncontrolled and controlled vehicle was obtained and compared [**21**].

One of the areas where bond graphs are widely used is Mechatronics. The role of Bond graph modelling in mechatronic systems have been presented in [**22**] in which approach for both linear and non linear systems was discussed. Piezoelectric sensors, operational amplifiers, rotational actuators and thermo-fluid systems were modelled and simulated by integrating with SIMULINK. A simple drive illustrating torsional resonance was modelled in [**23**] leading to the modelling of three coupled electric drives of different configurations. A two link rigid arm with drive flexibility was successfully modelled.

Another area where Bond graph has found acceptance is multi body dynamics. A multi body dynamic system has been modelled in [**24**] and a multi body system with kinematic loops has been presented in [**25**]. Bond graphs have also been used for identification [**26**] and fault detection [**27**]. Hardware-in-loop dynamics simulator has also been modelled in this environment [**28**].

2.2 Literature Gap

Based on the literature survey carried out following gaps have been identified:

- Very few trajectories tracking model of the 3-DOF parallel planar manipulator with electrically actuated manipulator leg has been developed
- Target reaching model of the same manipulator has not been reported in the literature
- Very few workspace analysis technique of the parallel manipulator has been reported in literature

2.3 Objectives of the Present Work

Based on the literature gaps identified in the previous section the objectives of this thesis dissertation are:

- To model a ball screw feed drive as electrically actuated manipulator leg
- To develop a trajectory tracking model of a 3-DOF parallel planar manipulator
- To develop a target reaching model of a 3-DOF parallel planar manipulator
- To develop workspace analysis of the planar parallel manipulator

Chapter 3 Trajectory Tracking For Parallel Manipulator

This chapter deals with the construction and working of the 3 degree of freedom (DOF) parallel planar manipulator employed for trajectory tracking purposes. Ball screw feed drive which is used as leg of parallel manipulator to impart motion to it is also discussed. Bond graph models of the ball screw feed drive together with the manipulator and the inversion controller is also presented in this chapter.

3.1 Parallel Planar Manipulator

3.1.1 Introduction

Trajectory tracking essentially refers to replication of an input reference trajectory by the end effectors of the manipulator. Trajectory tracking finds wide applications in the world of manipulators be it machining, finishing, welding or a simple pick and place application. Replication of the input along given coordinates with negligible errors form the basic characteristic of a trajectory tracking system.

The schematic diagram of the parallel planar manipulator having 3-DOF is presented in Fig. 3.1. The manipulator consists of a moving platform AB supported by three prismatic legs 1, 2 and 3. The three prismatic legs are actuated by ball screw feed drive. These are connected to the platform with three moving un-actuated revolute joints whereas to the fixed base CDE with three fixed un-actuated revolute joints. The centre of gravity of the manipulator is assumed to lie at point G which is the midpoint of the platform. θ_G is the angle that the platform makes with the horizontal axis.

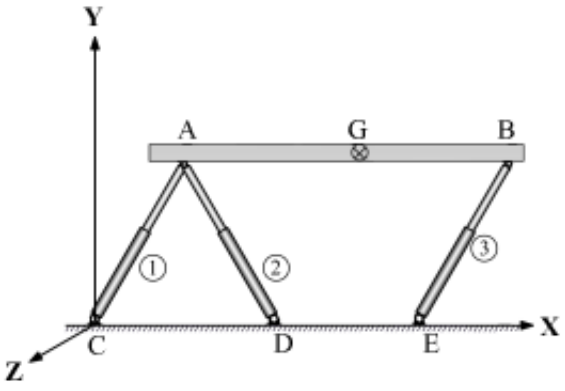

Fig. 3.1 Schema of the parallel planar manipulator

3.1.2 Ball Screw Feed Drive

Ball screw feed drives find wide acceptance and applications in industry due to their positional accuracy and mechanical efficiency. These are used as prismatic joints in the manipulator legs by virtue of their ability to convert rotational motion into linear motion. The schematic diagram of a typical ball screw used as a prismatic leg is presented in Fig. 3.2. It consists of a motor connected through a coupling to a threaded shaft which is supported by bearings fixed to base. As torque is applied to the motor, the rotation of the shaft produces linear motion as a result of threads and screw action on the link and supported by nut. The mechanical equivalent of the assembly is depicted in Fig. 3.3. In this, the various components are represented as masses, springs and dampers [**30**]. For simplicity the characteristics of the shaft are segregated into linear and rotational branches. The parameters in the model shown like mass of the link m_t, mass of the ball screw shaft m_s, rotary inertia of shaft J_s and motor J_m and various rigidity and damping factors denote their physical values.

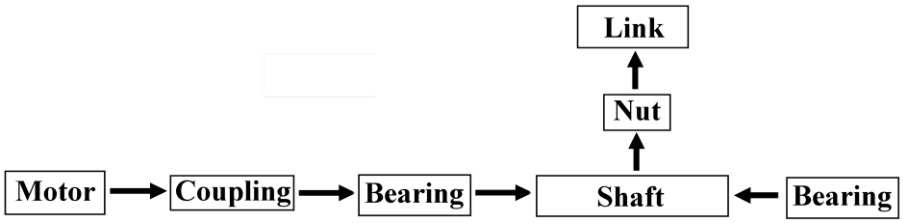

Fig. 3.2 Schematic diagram of ball screw feed drive prismatic leg

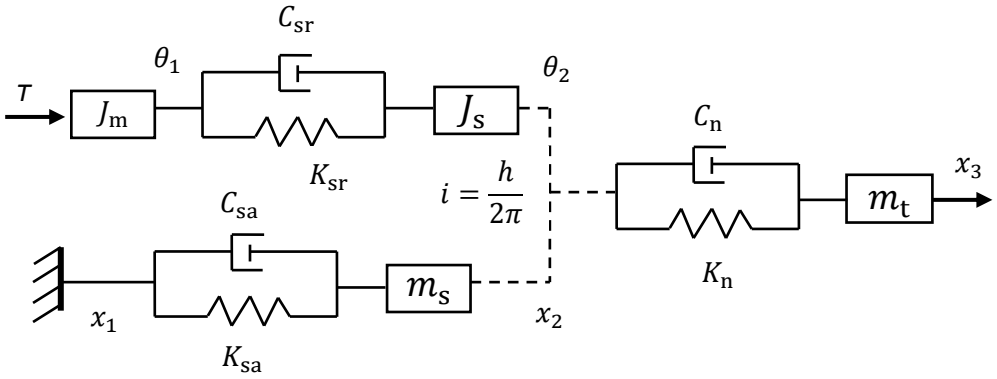

Fig. 3.3 Mechanical equivalent of ball screw feed drive prismatic leg

The axial and rotational stiffness of shaft are given by

$$k_{sa} = \frac{\pi^2}{4l_{eff}} d^2 E \tag{3.1}$$

$$k_{\mathrm{sr}} = \frac{\pi}{32} d^4 l \rho (2\pi f_{\mathrm{s}})^2 \tag{3.2}$$

$$f_{\mathrm{s}} = \frac{1}{4l}\sqrt{\frac{G}{\rho}} \tag{3.3}$$

where k_{sa} and k_{sr} being the axial and radial stiffness, *E* Young's modulus, *G* shear modulus and ρ density of the shaft. Symbols l_{eff}, l and d represent the effective length, total length and equivalent diameter of the shaft. f_{s} is the eigenfrequency of the shaft [**2**]. The rigidity values of coupling, bearing and shaft are combined to obtain the overall axial k_{a} and rotational k_{r} rigidity values of the system which are given as

$$k_{\mathrm{a}} = \left(\frac{1}{k_{sa}} + \frac{1}{k_{\mathrm{b}}}\right)^{-1} \tag{3.4}$$

$$k_{\mathrm{r}} = \left(\frac{1}{k_{\mathrm{sr}}} + \frac{1}{k_{\mathrm{c}}}\right)^{-1} \tag{3.5}$$

where k_{sa} and k_{sr} are the axial and rotational stiffness of the shaft respectively and whereas k_b is the axial stiffness of the bearing and k_{c} is the rotational stiffness of the coupling.

3.1.3 Overwhelming Control

The greatest challenge while developing an inverse controller of a plant is to estimate various characteristic such as un-modelled inertia, friction, backlash, etc. which continuously change with time. The strategy to deal with this challenge is to develop such robust controllers which are least sensitive to the concerned parameters. Overwhelming control is one such method to deal with the parameter uncertainties. In an overwhelming control, the controller mass M^* is rigidly attached to the plant mass in physical domain and it drags the plant mass together with itself. The plant dynamics are completely overwhelmed by the controller dynamics by the application of a high gain, $\mu_{\mathrm{H}} >> 1$ at the same maintaining the similarity of motion with the plant by the application of a low gain, $\mu_{\mathrm{L}} = 1$. Consequently, the dynamics of plant mass become a small perturbation on controller dynamics. In an overwhelming control, the controller parameters are focused upon to generate the desired plant performance.

3.2 Bond Graph Modelling

Based on the construction and working of the parallel planar manipulator with ball screw feed drive discussed in the previous section, bond graph models of the parallel manipulator with ball screw feed drive and trajectory tracking system are developed.

3.2.1 Parallel Planar Manipulator

Fig. 3.4 presents the bond graph model of the parallel planar manipulator with 3 DOF. In this model, the linear velocities of centre of gravity, i.e. point G in *x*-*y* plane ($\dot{x}_{\mathrm{G}}, \dot{y}_{\mathrm{G}}$) and rotational velocity about *z* axis ($\dot{\theta}_{\mathrm{G}}$) are used to define the velocities of points A and B which are

$$\dot{x}_{\mathrm{A}} = \dot{x}_{\mathrm{G}} + S_1 \dot{\theta}_{\mathrm{G}} \sin\theta_{\mathrm{G}} \tag{3.6}$$

$$\dot{y}_{\mathrm{A}} = \dot{y}_{\mathrm{G}} - S_1 \dot{\theta}_{\mathrm{G}} \cos\theta_{\mathrm{G}} \tag{3.7}$$

$$\dot{x}_{\mathrm{B}} = \dot{x}_{\mathrm{G}} - S_2 \dot{\theta}_{\mathrm{G}} \sin\theta_{\mathrm{G}} \tag{3.8}$$

$$\dot{y}_{\mathrm{B}} = \dot{y}_{\mathrm{G}} + S_2 \dot{\theta}_{\mathrm{G}} \cos\theta_{\mathrm{G}} \tag{3.9}$$

where S_1 and S_2 are lengths of AG and GB respectively. The junction pairs ($1_{\dot{x}_{\mathrm{A}}}, 1_{\dot{y}_{\mathrm{A}}}$) and ($1_{\dot{x}_{\mathrm{B}}}, 1_{\dot{x}_{\mathrm{B}}}$) represent the velocities of points A and B, respectively whereas I-elements connected to the velocities of centre of gravity, point G represent the mass (M_{P}) and moment of Inertia (J_{P}) of the platform. A source of effort connected to $1_{\dot{y}_{\mathrm{G}}}$ junction models the weight of the platform. The flow detectors added to velocities of point G are used to modulate the modulated transformer elements in order to satisfy the kinematics of the moving platform. The leg lengths represented by $1_{\dot{l}_{\mathrm{ac}_1}}$, $1_{\dot{l}_{\mathrm{ac}_2}}$ and $1_{\dot{l}_{\mathrm{ac}_3}}$ are modelled as per plane impedance model with relevant modulated transformers. The generalized form of leg lengths can be expressed as

$$l_{\mathrm{ac}}^2 = (x_2 - x_1)^2 + (y_2 - y_1)^2 \tag{3.10}$$

Differentiating this with respect to time gives

$$\dot{l}_{\mathrm{ac}} = \left(\frac{x_2 - x_1}{l_{\mathrm{ac}}}\right)(\dot{x}_2 - \dot{x}_1) + \left(\frac{y_2 - y_1}{l_{\mathrm{ac}}}\right)(\dot{y}_2 - \dot{y}_1) \tag{3.11}$$

where (x_1, y_1) and (x_2, y_2) are the coordinates of the two ends of the leg. The input to the platform model is the effort to the actuator legs and output is the motion of the platform.

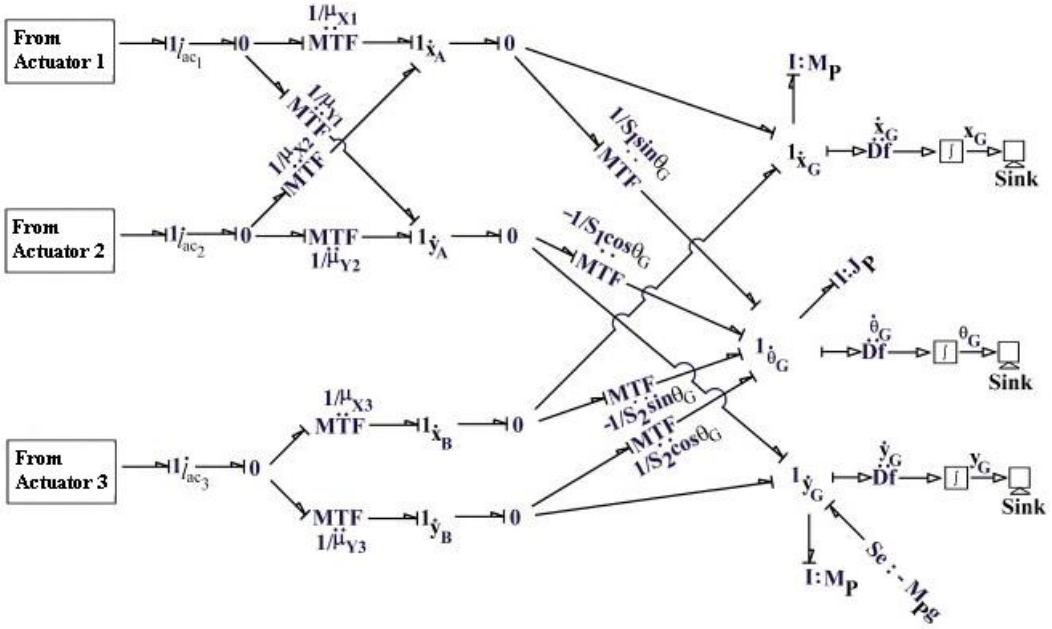

Fig. 3.4 Bond graph model of planar platform

3.2.2 Ball Screw Feed Drive

Figure 3.5 shows the forward model of ball screw feed drive which is developed as per the mechanical equivalent of the typical drive as discussed in Section 3.1.2. Junctions $1_{\dot{\theta}_1}$ and $1_{\dot{\theta}_2}$ represent the angular velocities of motor and shaft respectively. I and R-elements connected to these two junctions represent corresponding values of moment of inertia (J_{m},J_{P}) and damping coefficients (R_{m}). The C-element with stiffness parameter k_{r} and R-element with damping parameter C_{r} which are in mechanical parallel with each other represent the stiffness and damping of the rotational component of the system. Similarly, the C-element with stiffness parameter k_{a} and R-element with damping parameter C_{a} represent the stiffness and damping of the translational component of the system. The angular velocity of the shaft is transformed into linear velocity by transformer element and added with the translational velocity which is represented by $1_{\dot{x}_4}$-junction. The C and R-elements with stiffness and damping parameters k_{n} and C_{n} are used to model the nut so as to generate the motion of the link represented by $1_{\dot{x}_4}$ junction to which an I-element with parameter m_{t} is connected. The input to the system is the applied torque to the motor whereas the output of the system is the motion of the moving platform.

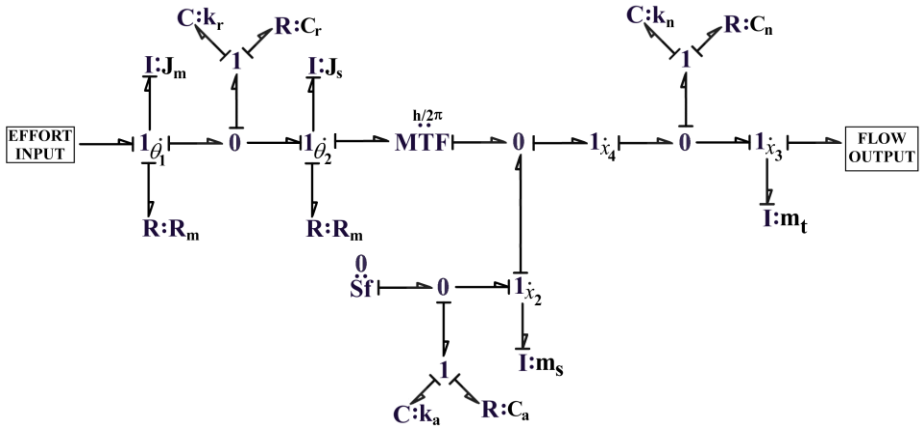

Fig. 3.5 Forward model of ball screw feed drive

The inverse model of the ball screw feed drive is shown in Fig. 3.6. In the inverse model all the physical parameters, relations and connections between the different elements are same as in the forward model. The power directions of the bonds have been reversed and the model is redrawn. The input to the inverse model is the effort at the link whereas output of the system is angular velocity of the motor.

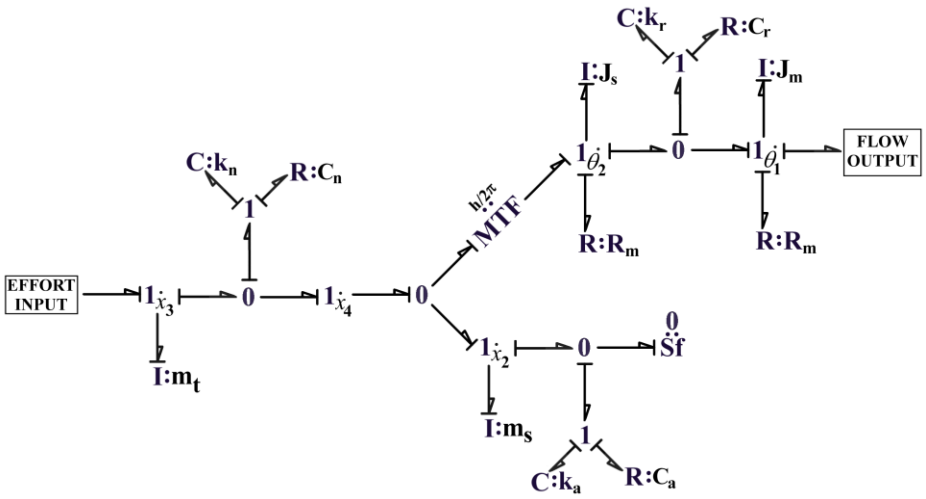

Fig. 3.6 Inverse model of the ball screw feed drive

3.2.3 Parallel Manipulator with Ball Screw

Figure 3.7 shows the word bond graph of the parallel planar manipulator with ball screw for trajectory tracking purpose. It consists of two sub models named controller and plant. The reference velocities in *x* and *y* are input to the controller by two source of flows. The controller

generates the required efforts which is then fed into the three legs of the plant so as to successfully track the given reference trajectories.

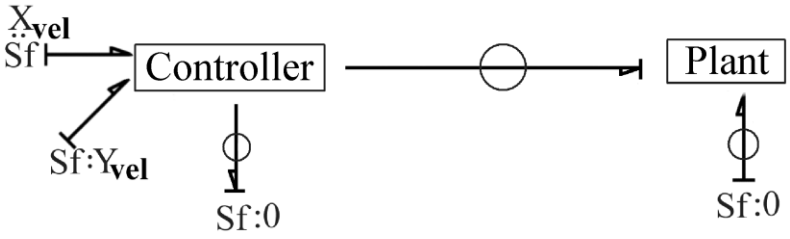

Fig. 3.7 Word bond graph of parallel manipulator

The bond graph of the plant is depicted in Fig. 3.8. Plant model also known as forward model is essentially the platform model as developed in Section 3.2.1 together with legs actuated by ball screw feed drive which gets input from the inversion controller after the plant dynamics are overwhelmed by the high gain, μ_H by the overwhelming controller. Low gain, μ_L of value equal to one ensures that the plant exactly executes the motion input to the controller. The forward model of ball screw feed drive modelled in the previous section is represented as BS. Pad stiffness and damping elements are added after BS sub model to avoid differential causality. The input to this model is the effort received from the inverse model and the output is the motion of the platform together with the flow supplied to inverse model or controller.

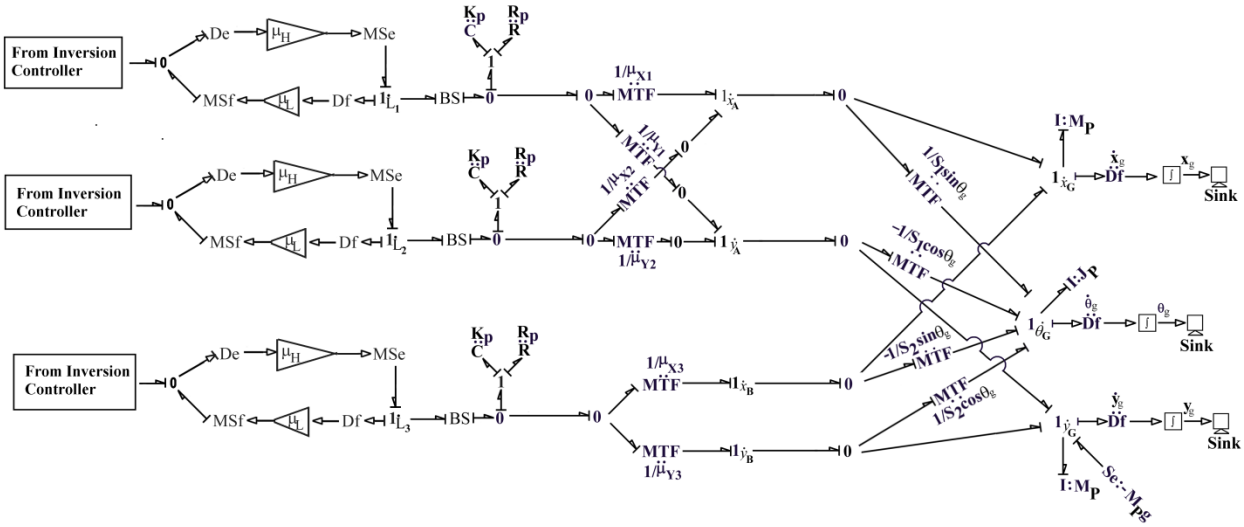

Fig. 3.8 Forward model of the manipulator

Figure 3.9 shows the inverse model of the manipulator. Inverse model in controller domain is essentially the mirror image of the forward model together with modifications carried out to

make it computationally suitable. Junctions $1_{\dot{x}_A}$ and $1_{\dot{x}_A}$ which represent the linear velocities of point A have been dissociated into two pairs. The inverse model of ball screw feed drive as modelled in Section 3.2.2 is shown as a sub model INV-BS. Stiff pads having C and R-elements in mechanical parallel to each other have been added before velocities of centre of gravity ($1_{\dot{x}_G}$, $1_{\dot{y}_G}$ and $1_{\dot{\theta}_G}$) and INV-BS sub model to avoid differential causality. C-elements added after INV-BS sub model return effort to the forward model. The reference trajectory desired to be tracked is fed through three source of flows attached to the three 1-junctions ($1_{\dot{x}_G}$, $1_{\dot{y}_G}$ and $1_{\dot{\theta}_G}$) representing velocities of the centre of gravity through stiff pads. The input to the inverse model is flow from three sources of flows and flow received in feedback from the forward model and output is the force supplied to the forward model.

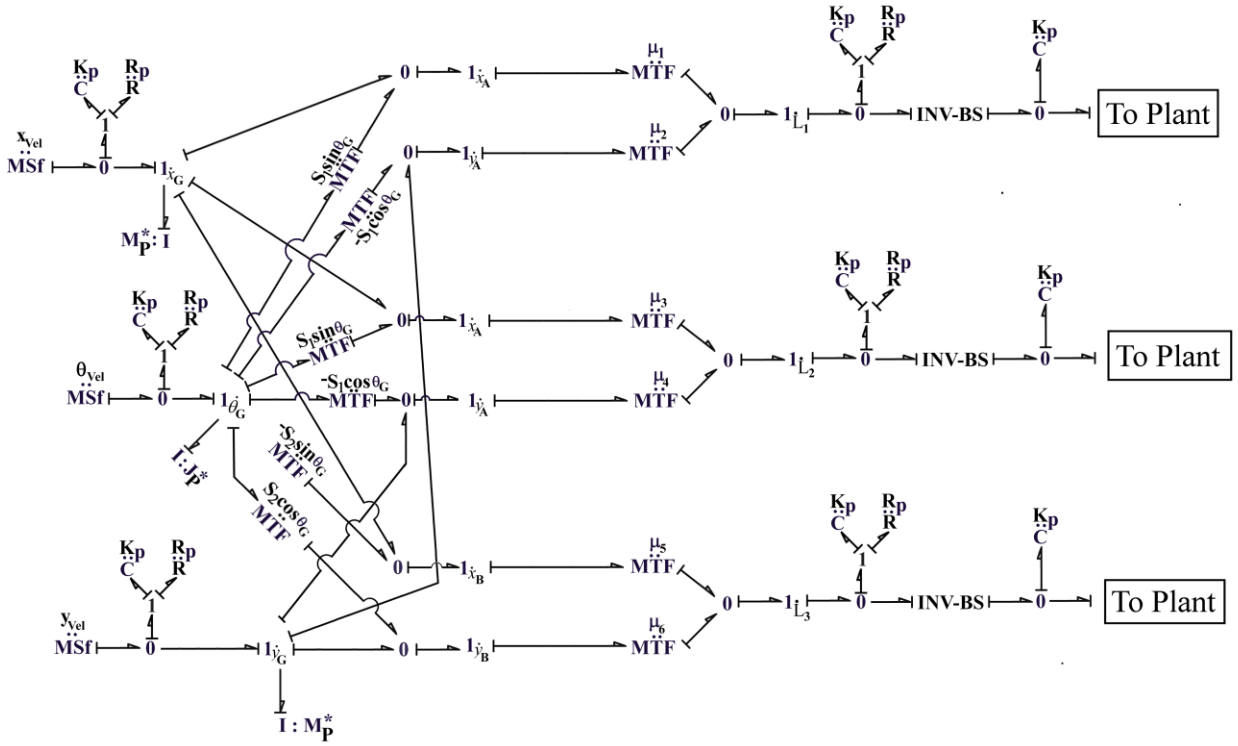

Fig. 3.9 Inverse model of the manipulator

3.3 Parameter Values and Simulation Results

This section deals with the various results obtained from the simulations carried out on the full model of Parallel manipulator. Results for trajectory tracking were obtained by running bond graph model simulations on software named SYMBOLS SHAKTI.

Some of the parameters related with the systems are taken from reference [**30**] and others have been chosen accordingly. The different parameters selected for simulations are provided in Table 3.1. The initial configuration of the manipulator is specified in Table 3.2. In the initial position, links 1, 2 and 3 are of length 1.118 m each and make angles of 1.10715, 2.0344 and 1.0715 rad respectively with the horizontal axis.

Table 3.1 Parameter Values

Sub systems	Parameter values			
Platform	$M_{\mathrm{P}} = 11\,\mathrm{kg}$	$J_{\mathrm{P}} = 0.1\,\mathrm{kg\,m^2}$	$K_{\mathrm{j}} = 10^8\,\mathrm{N/m}$	$R_{\mathrm{j}} = 50\ \mathrm{Ns/m}$
Ball screw feed drive	$h = 0.02\,\mathrm{m}$	$J_{\mathrm{m}} = 6.4\mathrm{e}^{-3}\,\mathrm{kg\,m^2}$	$J_{\mathrm{s}} = 6.5\mathrm{e}^{-4}\,\mathrm{kg\,m^2}$	$l = 2\,\mathrm{m}$
	$k_{\mathrm{c}} = 141\mathrm{e}^{3}\,\mathrm{Nm/mrad}$	$d = 0.038\,\mathrm{m}$	$C_{\mathrm{c}} = 0.01\,\mathrm{Ns/m}$	$C_{\mathrm{sr}} = 0.01\,\mathrm{Ns/m}$
	$k_{\mathrm{b}} = 250\mathrm{e}^{6}\ \mathrm{N/m}$	$k_{\mathrm{n}} = 500\mathrm{e}^{6}\ \mathrm{N/m}$	$r_{\mathrm{m}} = 0.01\,\mathrm{Ns/m}$	$R_{\mathrm{n}} = 0.01\,\mathrm{Ns/m}$
	$k_{\mathrm{r}} = 50\ \mathrm{Ns/m}$	$k_{\mathrm{a}} = 50\ \mathrm{Ns/m}$	$m_{\mathrm{s}} = 1\,\mathrm{kg}$	$m_{\mathrm{t}} = 11\,\mathrm{kg}$
Inverse system	$M^{*}_{\mathrm{p}} = 11\,\mathrm{kg}$	$J^{*}_{\mathrm{p}} = 0.1\,\mathrm{kg\,m^2}$	$K_{\mathrm{c}} = 10^8\ \mathrm{N/m}$	$R_{\mathrm{c}} = 50\ \mathrm{Ns/m}$

The bond graph simulation for trajectory tracking model is run for t = 6.28 s. The reference trajectory or command is a double semi circle denoted by Fig. 3.10(a). The two source of flows along x and y axes so as to generate the first semi circle for t = 0 to $\frac{\pi}{\omega}$ are as follows

$$\dot{x} = -r\omega \sin(\omega t) \tag{3.12}$$

$$\dot{y} = r\omega \cos(\omega t) \tag{3.13}$$

Table 3.2 Initial condition of the manipulator

Points	x	y
A	0.5 m	1 m
G	1.5 m	1 m
B	2.5 m	1 m
C	0 m	0 m
D	1 m	0 m
E	2 m	0 m

whereas for t = $\frac{\pi}{\omega}$ to $\frac{2\pi}{\omega}$, the source of flows along x and y axes are as

$$\dot{x} = -r\omega \sin\left(\omega\left(t - \frac{\pi}{\omega}\right)\right) \tag{3.14}$$

$$\dot{y} = r\omega \cos\left(\omega\left(t - \frac{\pi}{\omega}\right)\right) \tag{3.15}$$

where ω and r are angular frequency and radius of the semi circle having values of 1 rad/s and 0.1 m respectively.

The command or reference trajectory is shown in Fig. 3.10(a) whereas the response or the motion of centre of gravity of the platform is shown in Fig. 3.10(b). It can be seen from Fig. 3.11 that the manipulator successfully tracks the given command. The centre of gravity of the platform starts from its initial position of (1.5, 1) m and completes the first semi circle at t = π s at (1.3, 1) m and the second at t = 2π reaching (1.1, 1) m.

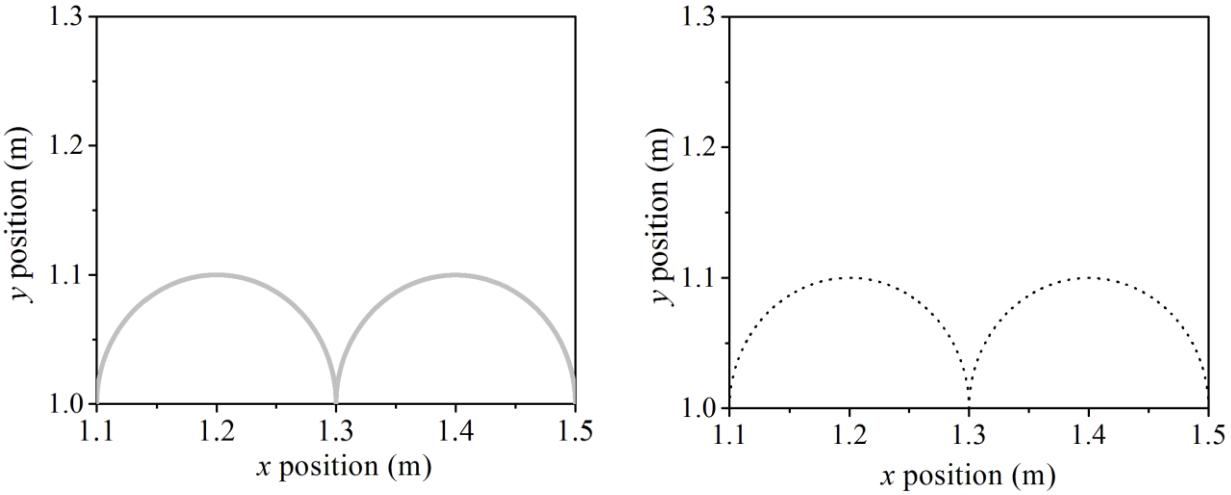

Fig. 3.10 Plot of y position with x position of (a) command and (b) response

Figure 3.12 depicts the change in lengths and angles from x axis of the three actuators. The initial lengths of the legs are taken to be 1.118 m each and leg angles with x direction are 1.10715, 2.0344 and 1.0715 rad. At the final position when the manipulator reaches the target the leg lengths are 1.00531, 1.34559 and 1.00531 and leg angles are 1.47116, 2.30184 and 1.47116 rad. The change in leg lengths and leg angles is within 0.3 m and 0.4 rad respectively for the complete motion of the manipulator. The leg lengths and the leg angles of all the three legs change as per the movement of the platform.

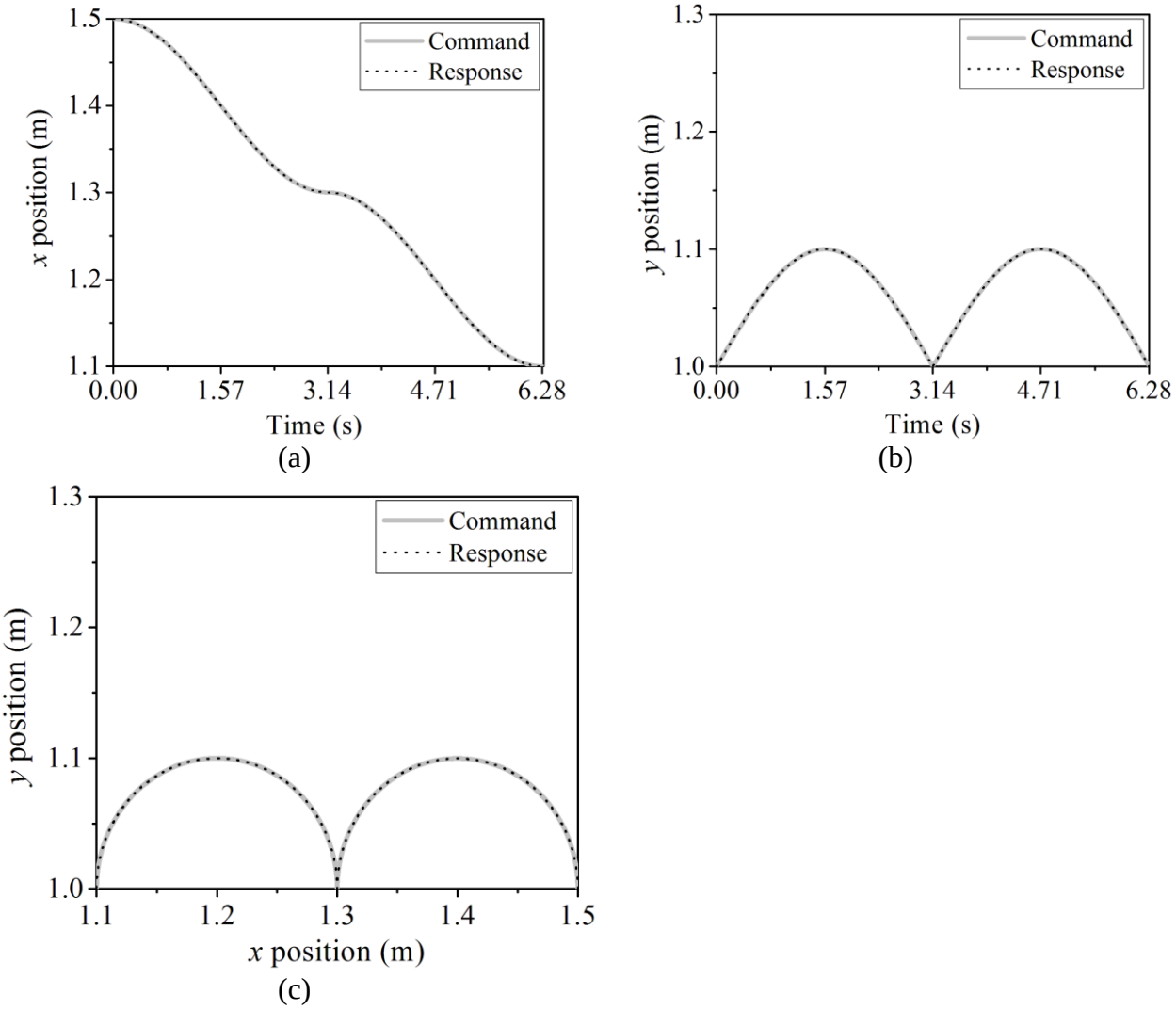

Fig. 3.11 Simulator performance in replicating (a) x position (b) y position with time and (c) y position with x position

It may be noted that the nature of change of leg lengths and leg angles is replicated for the second semi circle after t = $\frac{\pi}{\omega}$ s. Also, as there is no rotation of the platform, motions of legs 1 and 3 are identical. The cusp appearing in the plot of leg lengths is due to sudden change in the gradient of the trajectory at the completion of the first semi circle.

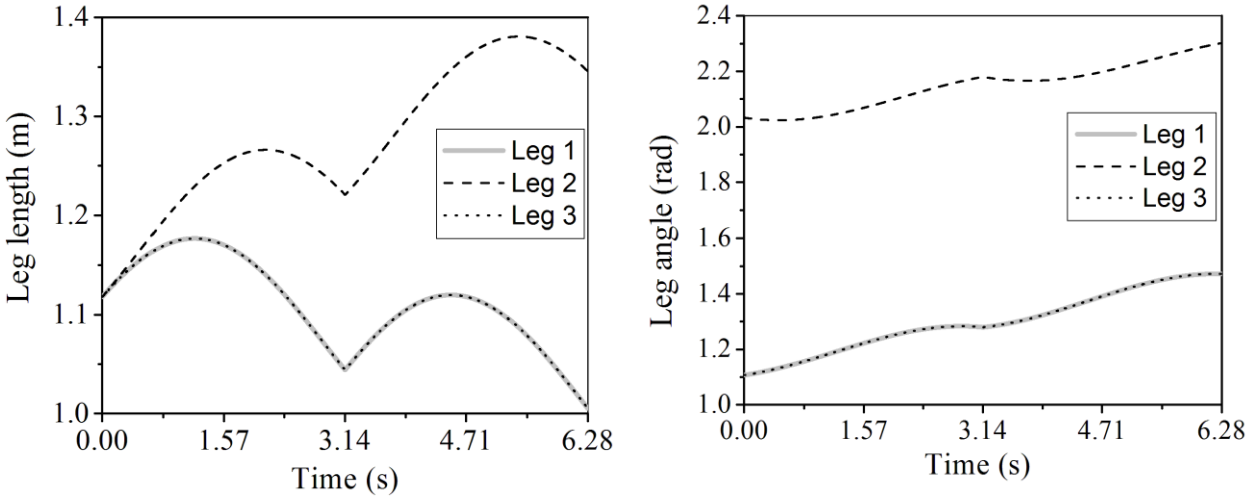

(a) (b)

Fig. 3.12 Change in (a) lengths and (b) angles of actuators 1, 2 and 3

Figure 3.13 shows the absolute error in tracking x and y positions of the reference trajectory. The absolute errors in tracking x and y positions are within ± 9.1×10^{-5} m and ± 1.3×10^{-4} m respectively. Figure 3.14 shows the percentage error in tracking x and y positions of the reference trajectory. The percentage errors in x and y positions range within ± 0.007 and ± 0.0135 respectively. The maximum error is observed at t = $\frac{\pi}{\omega}$ s where there is steep change in gradient.

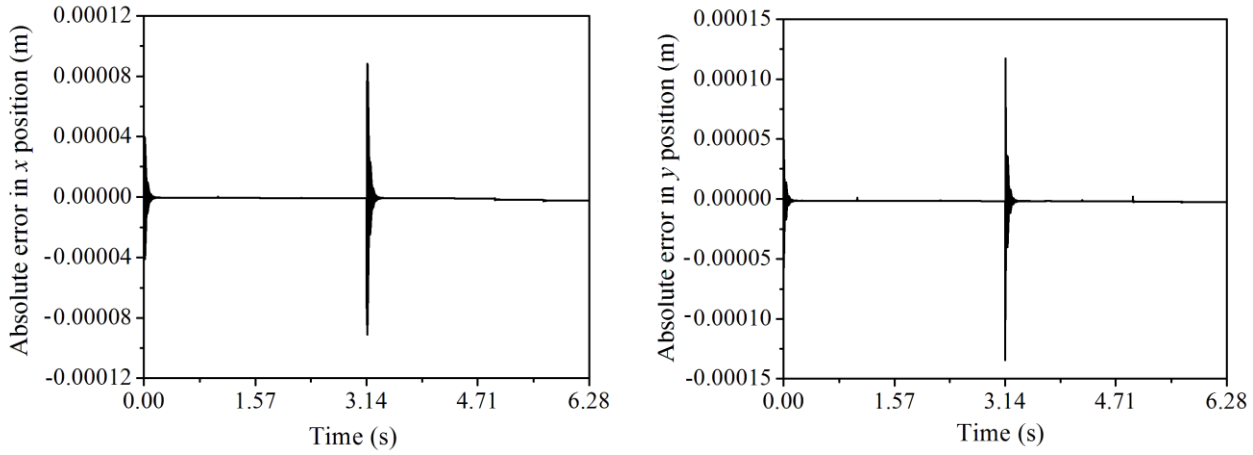

(a) (b)

Fig. 3.13 Absolute error in tracking (a) x position and (b) y position

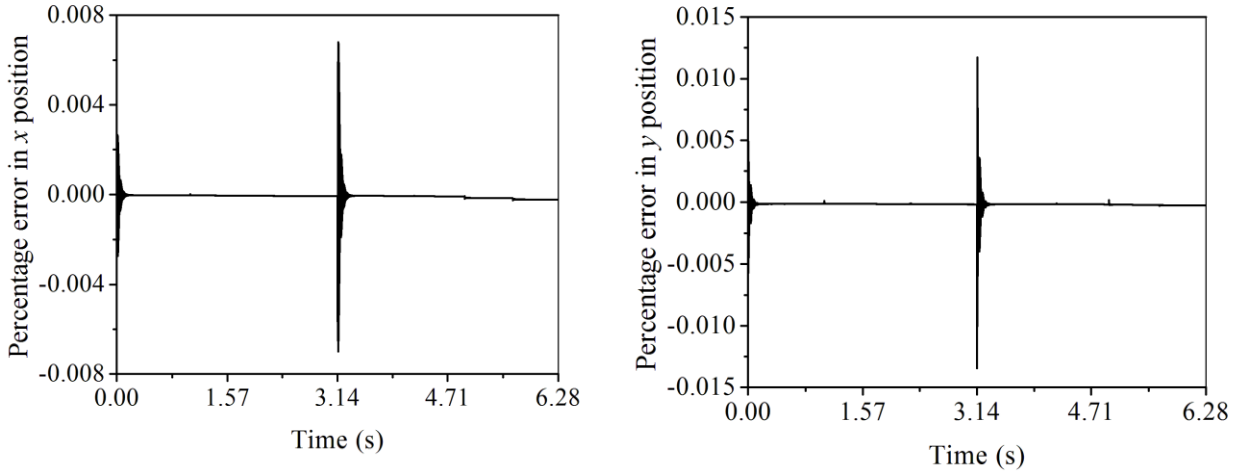

(a) (b)

Fig. 3.14 Percentage error in tracking (a) x position and (b) y position

Chapter 4 Target Reaching and Workspace Analysis

This chapter deals with the construction and working of a 3 degree of freedom planar parallel manipulator employed for point to point motion or reaching at a given target. Ball screw feed drive which is used to impart motion to the manipulator is discussed. Ball screw feed drive together with the manipulator and the inversion controller is modelled. Workspace analysis associated with the manipulator is done at the end of the chapter.

4.1 Introduction

4.1.1 Parallel Planar Manipulator

The manipulator under consideration is a 3-DOF parallel planar manipulator. The manipulator consists of a moving platform supported by three prismatic joints actuated by ball screw feed drive which is connected to the fixed base and moving platform with unactuated revolute joints. The same has been described in Section 3.1.1.

4.1.2 Ball Screw Feed Drive

Ball screw feed drives have been used as prismatic joints in the manipulator legs by virtue of their ability to convert rotational motion into linear motion. It consists of a motor connected through a coupling to a threaded shaft which is supported by bearings fixed to base. As torque is applied to the motor, the rotation of the shaft produces linear motion as a result of screw and thread action in the link mounted on it and supported by a nut. The same has been discussed in Section 3.1.2 in detail.

4.1.3 Target Reaching

Target reaching is the event of the end effector of the manipulator arriving or reaching at a given target. The target is usually fed in terms of its coordinates and the manipulator is required to reach the given target irrespective of the path traversed to reach it. The basic characteristic of a target reaching system is reaching at the given target with negligible errors.

4.1.4 Workspace Analysis

For determining the workspace of the 3-DOF planar parallel manipulator, the methodology given in reference [**11**] is followed. An inertial Cartesian frame O_{XY} is attached to point C of the manipulator with its *x*-axis parallel to the horizontal. Another non-inertial Cartesian frame $O_{X'Y'}$

is attached to the centre of gravity of the manipulator with *x*-axis parallel to the platform and subtending angle ϕ with the horizontal. The coordinates of fixed revolute joints expressed in inertial frame O_{XY} are $(x_{a_\mathrm{i}}, y_{a_\mathrm{i}})$ and the coordinates of moving revolute joints expressed in non inertial frame $O_{\mathrm{X'Y'}}$ are $(x_{b_\mathrm{i}}, y_{b_\mathrm{i}})$. The coordinates of centre of gravity in inertial frame are (*x, y,* ϕ). For a given position and orientation of the platform, leg lengths, L_i (*i*=1, 2, 3) of the manipulator can be expressed as

$$L_\mathrm{i}^2 = (x - x_{c_\mathrm{i}})^2 + (y - y_{c_\mathrm{i}})^2 \tag{4.1}$$

where

$$x_{c_\mathrm{i}} = x_{a_\mathrm{i}} - x_{b_\mathrm{i}} \cos\phi + y_{b_\mathrm{i}} \sin\phi \tag{4.2}$$

$$y_{c_\mathrm{i}} = y_{a_\mathrm{i}} - x_{b_\mathrm{i}} \sin\phi - y_{b_\mathrm{i}} \cos\phi \tag{4.3}$$

From these equations, it is evident that for a given orientation of the platform and without constraints on the unactuated joints, the workspace is obtained as the intersection of three pairs of concentric circles. The centres of the circles are $(x_{c_\mathrm{i}}, y_{c_\mathrm{i}})$ and minimum and maximum radii of each pair are L_i^{min} and L_i^{max}, respectively. The constraints on the fixed unactuated joints can be expressed as

$$\theta_{a_\mathrm{i}}^{min} \leq \theta_{a_\mathrm{i}} \leq \theta_{a_\mathrm{i}}^{max}, \qquad i = 1, 2, 3 \tag{4.4}$$

where θ_{a_i} is the angle subtended by the leg with horizontal. The imposition of the limits of each unactuated joint creates sectors on its corresponding annular region bounded by concentric circles. Finally, the required workspace is obtained as the intersection of the three zones of sectored annular regions.

4.2 Bond Graph Modelling

Based on the construction and working of the parallel planar manipulator with ball screw feed drive discussed in the previous sections, bond graph models of the parallel manipulator, ball screw feed drive and target reaching system are developed.

4.2.1 Parallel Planar Manipulator

In the bond graph model of parallel planar manipulator, the linear velocities of centre of gravity, i.e. point G are represented as $(1_{\dot{x}_\mathrm{G}}, 1_{\dot{y}_\mathrm{G}})$ and rotational velocity about *z* axis is represented as $1_{\dot{\theta}_\mathrm{A}}$. The junction pairs $(1_{\dot{x}_\mathrm{A}}, 1_{\dot{y}_\mathrm{A}})$ and $(1_{\dot{x}_\mathrm{B}}, 1_{\dot{y}_\mathrm{B}})$ represent the velocities of points A and B

respectively whereas I-elements connected to the velocities of centre of gravity, point G represent the mass(M_{P}) and moment of inertia (J_{P}) of the platform. A source of effort connected to $1_{\dot{y}_{\mathrm{G}}}$ junction models the weight of the platform. Modulated transformer elements are used in order to satisfy the kinematics of the moving platform. The same has been described in Section 3.2.1.

4.2.2 Ball Screw Feed Drive

In the bond graph model of ball screw feed drive Junctions $1_{\dot{\theta}_1}$ and $1_{\dot{\theta}_2}$ represent the angular velocities of motor and shaft, respectively. I and R-elements connected to these two junctions represent corresponding values of moment of inertia ($J_{\mathrm{m}}, J_{\mathrm{P}}$) and damping coefficients (R_{M}). The various C and R-elements which are in mechanical parallel to each other represent the stiffness and damping of corresponding components.

In the inverse model all the physical parameters, relations and connections between the different elements are same as in the forward model. The power directions of the bonds have been reversed and the model is redrawn. This is discussed in detail in Section 3.2.2.

4.2.3 Target Reaching

Figure 4.1 shows the word bond graph of the target reaching model. It consists of two sub models named controller and plant. The forces acting at the centre of gravity of the platform along x and *y* axes in order to make the manipulator reach the set target are input through two sources of effort. The controller or inverse model generates the required efforts which are then fed into the three legs of the plant so as to successfully reach the given target.

The bond graph of the plant is depicted in Fig. 4.2. Plant model also known as forward model is essentially the platform model as developed in Section 3.2.1 together with legs actuated by ball screw feed drive which gets input from the inversion controller. The forward model of ball screw feed drive modelled in the previous section is represented as ball screw (BS). Pad stiffness and damping elements are added after BS sub-model to avoid differential causality. The input to this model is the effort received from the inverse model and the output is the motion of the platform together with the flow supplied to inverse model or controller.

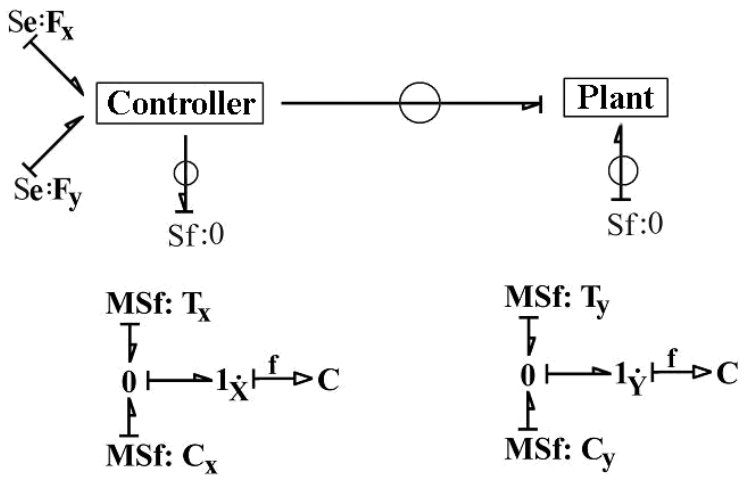

Fig. 4.1 Word bond graph of target reaching model

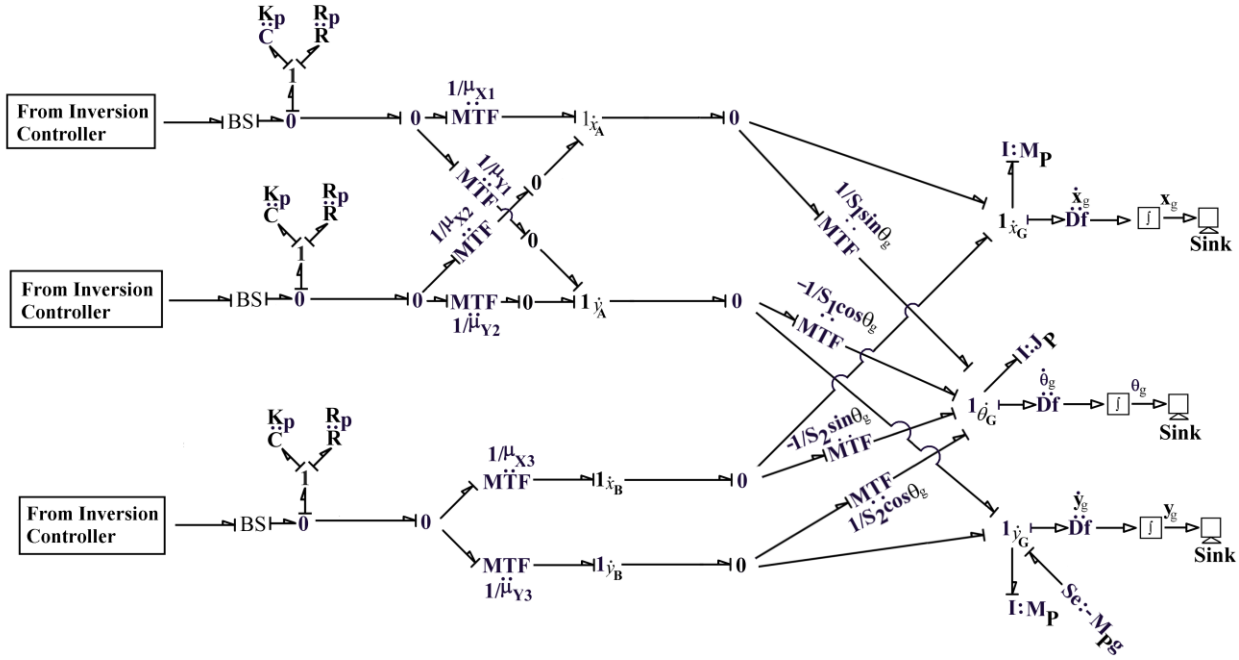

Fig. 4.2 Forward model of the manipulator

Figure 4.3 shows the inverse model of the target reaching system. Inverse model in controller domain is essentially the mirror image of the forward model together with modifications carried out to make it computationally suitable. Junctions $1_{\dot{x}_A}$ and $1_{\dot{y}_A}$ which represent the linear velocities of point A have been dissociated into two pairs. The inverse model of ball screw feed drive as modelled in Section 3.2.2 is shown as a sub model INV-BS. Stiff pads having C and R-

elements in mechanical parallel to each other have been added before INV-BS sub model to avoid differential causality. C-elements added after INV-BS sub model return effort to the forward model. The forces acting at the centre of gravity of the platform along *x* and *y* axes are input through two sources of effort. The input to the inverse model is forces applied along *x* and *y* direction and flow received in feedback from the forward model and output is the force supplied to the forward model.

The forces along *x* and *y*-axes which are input to the controller can be expressed as

$$F_{\mathrm{x}} = G_{\mathrm{x}} I \cos\theta \tag{4.5}$$

$$F_{\mathrm{y}} = G_{\mathrm{y}} I \sin\theta \tag{4.6}$$

where G_{x} and G_{y} are the corresponding gains and θ is the angle subtended by the line joining the target and the current positions with the *x*-axis. I is the input force. The current location is obtained by adding flow detectors to the centre of gravity in the forward model. The current *x* and *y* locations are subtracted into corresponding *x* and *y* target locations which are then fed by respective source of flows and the differences are obtained by adding flow detectors. The tangent of the angle θ is finally obtained by dividing the *y* difference in target and current positions to the *x* difference in target and current positions.

4.3 Parameter Values and Simulation Results

This section deals with the various results obtained from the simulations carried out on the full model of the target reaching manipulator. Results for target reaching were obtained by running bond graph model simulations on software named SYMBOLS SHAKTI whereas the results for workspace analysis were obtained on MATLAB.

4.3.1 Target Reaching

Some of the parameters related with the systems are taken from reference [**30**] and others have been chosen accordingly. The different parameters selected for simulations are provided in Table 4.1. The initial configuration of the manipulator is specified in Table 4.2. In the initial position, links 1, 2 and 3 are of length 1.118 m each and make angles of 1.10715, 2.0344 and 1.0715 rad , respectively with the horizontal axis.

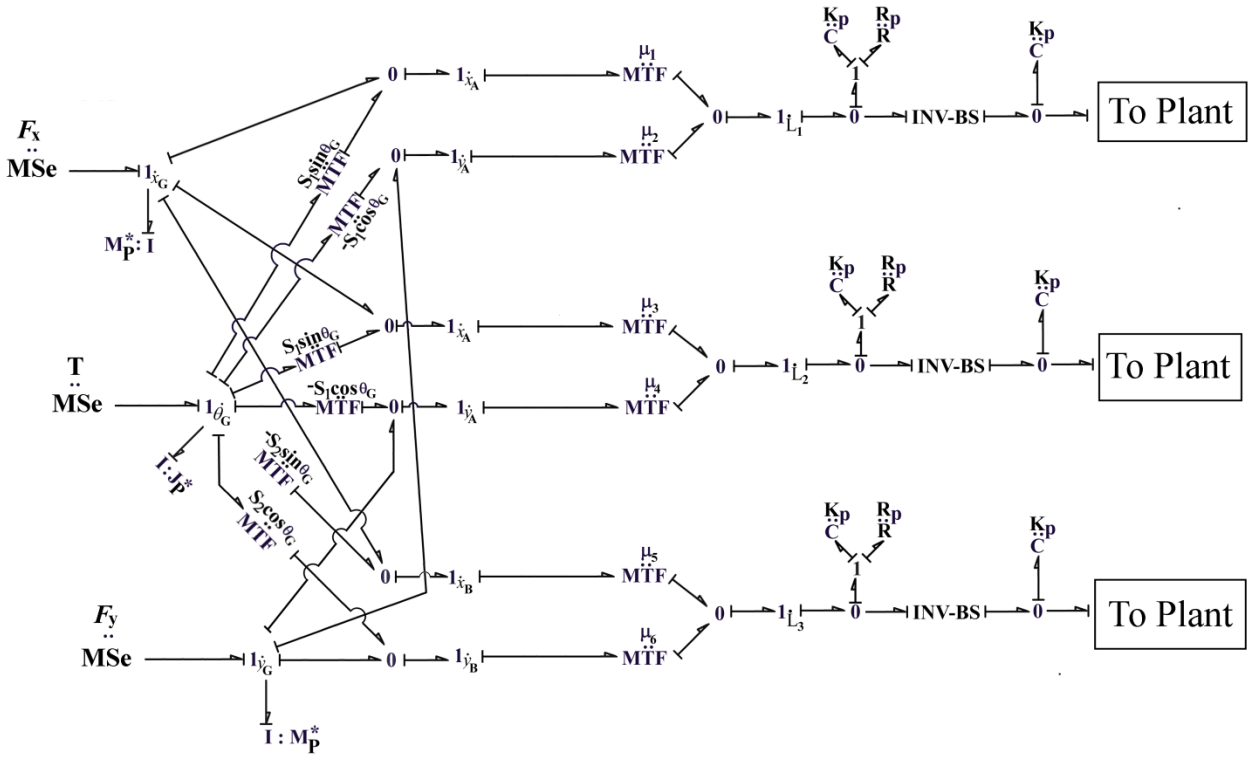

Fig. 4.3 Inverse model of the manipulator

The bond graph simulation for target reaching model is run for t = 8.92856 s. An initial disturbance along the direction of 1.6 rad from x axis is applied for t = 0.3 s following which the manipulator is allowed to move as per the algorithm. The target of (2.5, 3) is continuously fed through two source of flows. An input force of 10 N acts at the centre of gravity (G) with gain values of 64 and 60 in x and y directions, respectively. The manipulator continuously tracks the target at each time step and satisfactorily reaches the target (Fig. 4.4 (a), (b) and (c)). The initial and final locations are encircled and the arrow head denotes the direction of motion. The absolute errors in reaching the x and y coordinates of the target are 2.5×10^{-5} m and 1.6×10^{-4} m, respectively. The corresponding percentage errors are found to be 0.001 and 0.005. As evident from the figure, the centre of gravity of the manipulator starts from its initial position (1.5, 1) m and moves leftwards till the time the initial disturbance is in effect after which it starts turning towards the right and stabilizes so as to achieve an almost straight line path to finally reach its target located at (2.5, 3) m.

Figure 4.5 depicts the change in lengths and angles from the *x*-axis of the three actuators. The initial lengths of the legs are taken to be 1.118 m each and leg angles with x direction are 1.1071, 2.0344 and 1.0715 rad. At the final position when the manipulator reaches the target the leg lengths are 2.90715, 2.41136 and 3.91436 m and leg angles are 0.89502, 1.22451 and 1.26418 rad. The change in leg lengths and leg angles is within 3 m and 0.85 rad, respectively for the complete motion of the manipulator. The leg lengths and the leg angles of all the three legs change as per the movement as well as rotation of the platform.

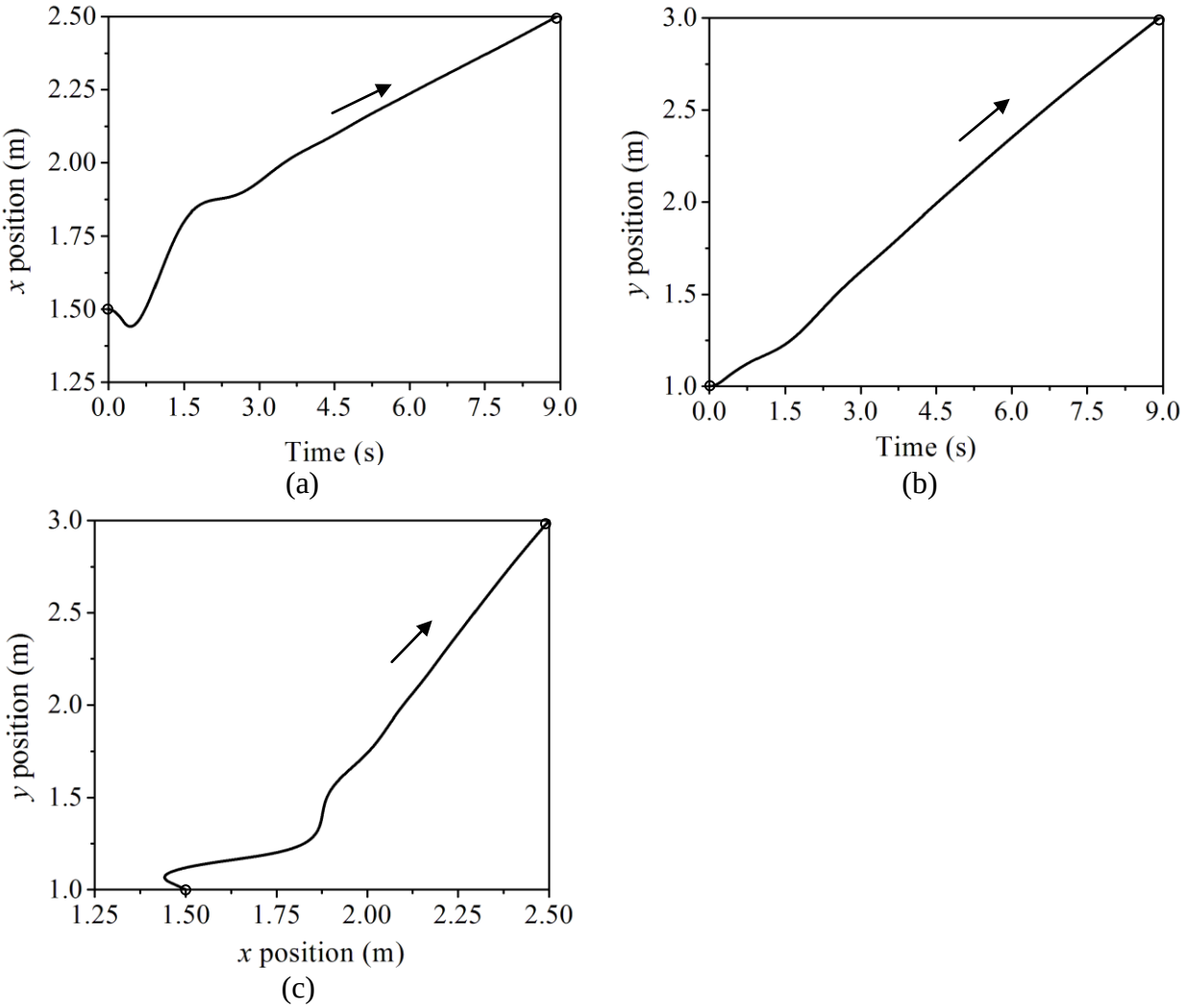

Fig. 4.4 Position of end effector in (a) y direction with time (b) x direction with time and (c) y with x direction

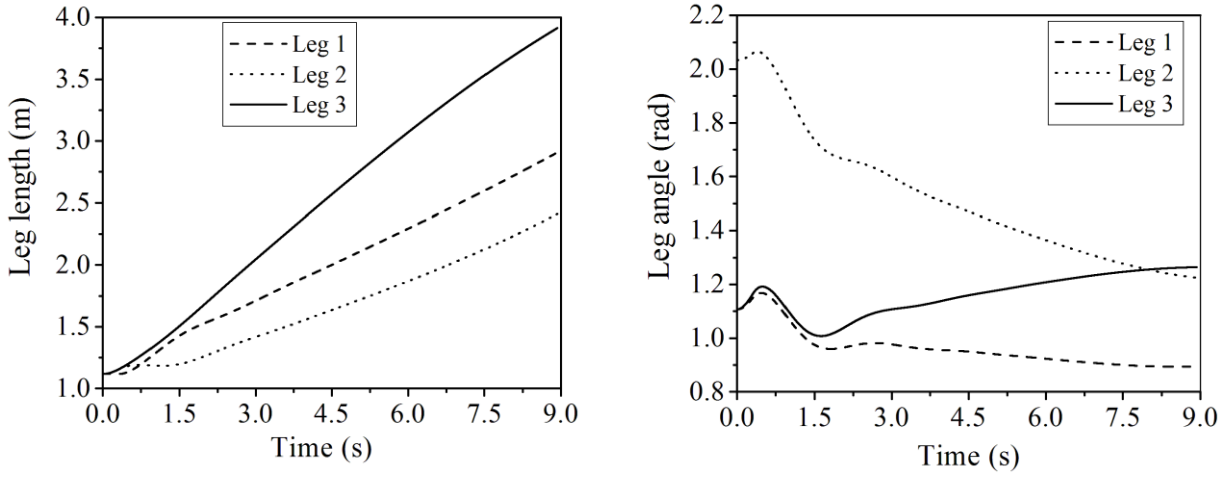

(a) (b)

Fig. 4.5 Change in (a) lengths and (b) angles of actuators 1, 2 and 3

4.3.2 Workspace Analysis

The workspace associated with the double semi circle trajectory tracked by the bond graph model discussed in Section 3.3 is determined and analyzed. The kinematic parameters together with joint limits were obtained from the trajectory tracking simulation and are listed in Table 4.1.

Table 4.1 Kinematic parameters and joint limits of the manipulator

i	1	2	3
x_{a_i} (m)	0	1	2
y_{a_i} (m)	0	0	0
x_{b_i} (m)	-1	-1	-1
y_{b_i} (m)	0	0	0
$L_i^{\min}$ (m)	1.00531	1.118	1.00531
$L_i^{\max}$ (m)	1.177	1.38071	1.177
$\theta_{a_i}^{\min}$ (rad)	1.10715	2.02377	1.10715
$\theta_{a_i}^{\max}$ (rad)	1.47163	2.30184	1.47163

The orientation of the platform is kept constant at zero radian and the simulation to determine the associated workspace is run on MATLAB. Shaded region in figure 4.6(a) denotes the workspace region without unactuated joint limits whereas 4.6(b) denotes the workspace with unactuated joints. The region ABCDEFGA in figure 4.6(c) which is the common region obtained by inter-section of various coloured arcs representing the joint limits represents the required workspace. The blue arc inside the workspace region is the trajectory starting at point F (1.5, 1) and terminating at point A (1.1, 1) is seen to aptly fit inside the workspace region hence validating the correctness of the result obtained. The area of the workspace region is determined by integrating its boundary between appropriate limits and is found to be 0.0553 m^2.

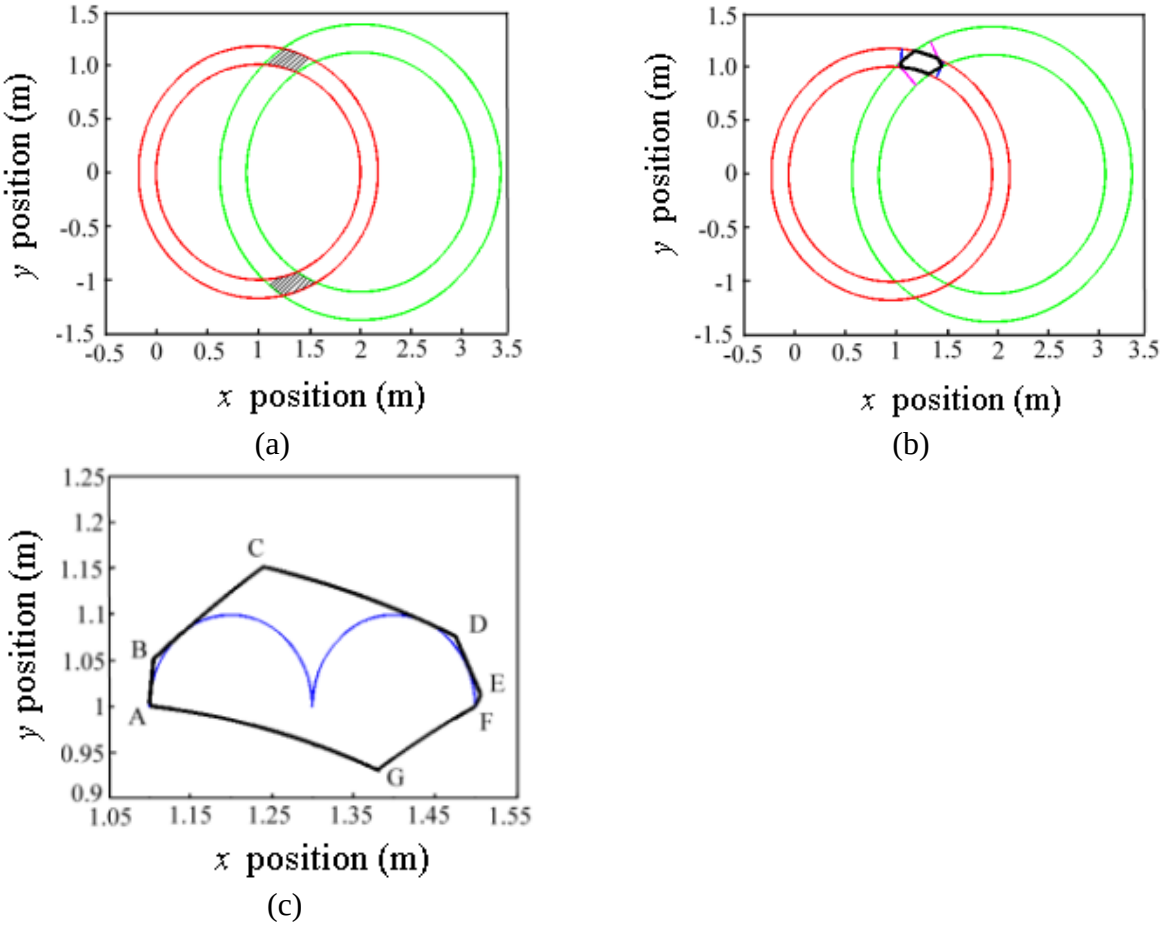

Fig. 4.6 Workspace associated with manipulator (a) without unactuated joint limits (b) with unactuated joint limits and (c) together with trajectory

Chapter 5 Conclusions

5.1 Conclusions

Based on the literature review and research work carried out as part of the dissertation work, following conclusions are drawn from this thesis:

- Parallel manipulators have higher load carrying capacity and stiffness but lesser workspace as compared to serial manipulators.
- Bond graph model of ball screw feed drive used as prismatic joint is developed.
- A parallel planar manipulator with ball screw feed drives employed as its legs is modelled.
- An inversion controller using overwhelming control for trajectory tracking purposes is developed and the manipulator is found to successfully track the given trajectory with negligible errors. The system also exhibits robustness against any parameter changing with time.
- Another inversion controller based on Proportional control is developed for target reaching purposes and the manipulator is found to successfully reach the given target with negligible errors.
- Workspace analysis associated with the trajectory tracking manipulator is carried out. Shape and minimum area of the workspace associated with trajectory tracked by the manipulator which should be kept clear of any foreign object so as to avoid any collision with the manipulator is obtained.

5.2 Scope for Future Work

- Revolute joints connecting the prismatic joints to the platform and the base may be modelled.
- Inversion controller for target reaching manipulator so as to keep the orientation of the platform constant may be developed.
- Workspace analysis was carried out assuming the orientation of the platform to be constant with time. Same may be carried out in case of variable platform orientation.
- Modelling of the 3-DOF parallel planar manipulator may be extended to 6-DOF parallel manipulators with workspace analysis.

REFERENCES

[1] Patel YD and George PM. Parallel manipulators applications–A survey. *Modern Mechanical Engineering* 2012; 2: 57–64.

[2] Dasgupta B and Mruthyunjaya TS. The Stewart platform manipulator: a review. *Mechanism and Machine Theory* 2000; 35: 15–40.

[3] Yildiz I and Omurlu VE. Reduced order dynamics and stability of a parallel manipulator through bond graph technique. In: *XXIII International Symposium on Information, Communication and Automation Technologies (ICAT),* Chicago, 2011.

[4] Wang X, Baron L and Cloutier G. Topology of serial and parallel manipulators and topological diagrams. *Mechanism and Machine Theory* 2008; 43: 754–770.

[5] Jun W, Tiemin L, Jinsong W and Liping W. Stiffness and natural frequency of a 3-DOF parallel manipulator with consideration of additional leg candidates. *Robotics and Autonomous Systems* 2013; 61: 868–875.

[6] Bera TK, Samantaray AK and Karmakar R. Robust overwhelming control of a hydraulically driven three-degrees-of-freedom parallel manipulator through a simplified fast inverse model. *Proceedings of the Institution of Mechanical Engineers, Part I: Journal of Systems and Control Engineering* 2010; 224: 169–184.

[7] Pathak PM, Kumar RP, Mukherjee A and Dasgupta A. A scheme for robust trajectory control of space robots. *Simulation Modelling Practice and Theory* 2008; 16: 1337–1349

[8] Bravo FG, Carbone G and Fortes JC. Collision free trajectory planning for hybrid manipulators. *Mechatronics* 2012; 22: 836–851.

[9] Gasparetto A and Zanotto V. A new method for smooth trajectory planning of robot manipulators. *Mechanism and Machine Theory* 2007; 42: 455–471.

[10] Tanev T. Workspace of hybrid (parallel-serial) robot manipulator. *Problems of Engineering Cybernetics and Robotics* 2006; 56.

[11] Gosselin CM and Jean M. Determination of the workspace of planar parallel manipulators with joint limits. *Robotics and Autonomous Systems* 1996; 17(3): 129-138.

[12] Merlet J, Gosselin CM and Mouly N. Workspaces of planar parallel manipulators. *Mechanism and Machine Theory* 1998; 33:7–20.

[13] Gosselin CM, Lemieux S and Merlet J. A new architecture of planar three-degree-of-freedom parallel manipulator. In: *Proceedings of the IEEE International conference on Robotics and Automation*, Minneapolis, Minnesota, April 1996.

[14] Gosselin C. Determination of the workspace of 6-DOF parallel manipulators. *Journal of Mechanical Design.* 1990; 112: 331–336.

[15] Hu B, Lu Y, Yu JJ and Zhuang S. Analyses of inverse kinematics, statics and workspace of a novel 3RPS-3SPR serial-parallel Manipulator. *The Open Mechanical Engineering Journal* 2012; 6: 65–72.

[16] Moosavian SAA, Nazari AA and Hasani A. Kinematics and workspace analysis of a novel 3-DOF spatial parallel robot. In: *19th Iranian Conference on Electrical Engineering*, 17 May, 2011.

[17] Ottaviano E and Ceccarelli M. Optimal design of capaman (cassino parallel manipulator) with prescribed workspace. In: *2nd Workshop on Computational Kinematics*, CK, May 2001.

[18] Dauphin TG, Rahmani A and Sueur C. Bond graph aided design of controlled systems. *Simulation Practice and Theory* 1999; 7: 493–513.

[19] Yildiz I, Omurlu VE and Sagirli A. Dynamic modeling of a generalized Stewart platform by bond graph method utilizing a novel spatial visualization technique. *International Review of Mechanical Engineering* 2008; 20.

[20] Kumar S, Kumar S and Singh CD. Modeling and simulation of underwater flexible manipulator as Raleigh beam using bond graph. *International Journal of Mechanical, Aerospace, Industrial, Mechatronic and Manufacturing Engineering* 2015; 9.

[21] Margolis D and Shim T. A bond graph model incorporating sensors, actuators, and vehicle dynamics for developing controllers for vehicle safety. *Journal of the Franklin Institute* 2001; 338: 21–34.

[22] Granda JJ. The role of bond graph modeling and simulation in mechatronics systems. *Mechatronics* 2002; 12: 1271–1295.

[23] Gawthrop PJ. Bond graphs: A representation for mechatronic systems. *Mechatronics* 1991; 1: 127–156.

[24] Cho W. A bond graph approach to the modelling of general multi body dynamic systems. *KSME International Journal* 1998; 12: 888–898.

[25] Favre W and Scavarda S. Bond graph representation of multi body systems with kinematic loops. *Journal of the Franklin Institute* 1998; 335B: 643–660.

[26] Gawthrop PJ, Jones RW and Mackenzie SA. Identification of partially known systems. *Automatica* 1992; 18: 831–836.

[27] Merzouki R, Medjaher K, Djeziri MA and Ould BB. Backlash fault detection in mechatronic system. *Mechatronics* 2007; 17: 299–310.

[28] Lin CF, Tseng CY and Tseng TW. A hardware in the loop dynamics simulator for motorcycle rapid controller prototyping. *Control Engineering Practice* 2006; 14: 1467–1476.

[29] Frey S, Dadalau A and Verl A. Expedient Modeling of Ball Screw Feed Drives. *Production Engineering* 2012; 6: 205–2011

CURRICULUM VITAE

Dharmveer Agarwal completed his BE in Mechanical Engineering from Birla Institute of Technology, Mesra, Ranchi, India in 2013. Thereafter, he worked as a service engineer with Caterpillar Inc. on CAT marine engines installed onboard Indian Navy and Indian Coast Guard ships where he got several opportunities to visit naval bases, ports, shipyards and workshops. He went on to pursue Master of Engineering in CAD/CAM Engineering at Thapar University, Patiala, India. His ME thesis is in the area of *Robotics and control*. He is preparing an international journal paper based on his dissertation work.

International Journal Publication:

1. Arora R, Agarwal D and Bera TK. "Target reaching and Workspace analysis of a hybrid manipulator", Simulation, IMechE, Sage Publisher. (**Under Preparation**)